



HAL
open science

Controlling nanoparticles dispersion in ionic liquids by tuning the pH

Clément Guibert, Vincent Dupuis, Jérôme Fresnais, Véronique Peyre

► **To cite this version:**

Clément Guibert, Vincent Dupuis, Jérôme Fresnais, Véronique Peyre. Controlling nanoparticles dispersion in ionic liquids by tuning the pH. *Journal of Colloid and Interface Science*, 2015, 454, pp.105-111. 10.1016/j.jcis.2015.04.059 . hal-01158520

HAL Id: hal-01158520

<https://hal.sorbonne-universite.fr/hal-01158520>

Submitted on 1 Jun 2015

HAL is a multi-disciplinary open access archive for the deposit and dissemination of scientific research documents, whether they are published or not. The documents may come from teaching and research institutions in France or abroad, or from public or private research centers.

L'archive ouverte pluridisciplinaire **HAL**, est destinée au dépôt et à la diffusion de documents scientifiques de niveau recherche, publiés ou non, émanant des établissements d'enseignement et de recherche français ou étrangers, des laboratoires publics ou privés.

Controlling nanoparticles dispersion in ionic liquids by tuning the pH

Clément GUIBERT, Vincent DUPUIS, Jérôme FRESNAIS, Véronique PEYRE*

Sorbonne Université, UPMC Univ Paris 06, UMR 8234, PHENIX, F-75005, Paris, France ;

CNRS, UMR 8234, F-75005, Paris, France.

Abstract

Hypothesis

Getting colloiddally stable dispersions of nanoparticles in ionic liquids is a challenging task. Indeed, long-range electrostatic repulsions often involved in molecular solvents are screened in ionic liquids and cannot counterbalance the interparticle attractions. Using a polyelectrolyte coating should provide a good stabilisation of the nanoparticles. Investigating the role of the polyelectrolyte charge on the dispersion state should yield to a better comprehension of the stabilisation mechanisms.

Experiments

Polyacrylate coated maghemite nanoparticles were transferred from water to ethylammonium nitrate, a protic ionic liquid, for various polymer chain length nanoparticles size. Titrations of coated nanoparticles and of free polymer chains were performed in water and in ethylammonium nitrate. The dispersion state of the nanoparticles was monitored at different pH by small-angle X-ray scattering.

Findings

Polyacrylate coating stabilised the nanoparticles in ethylammonium nitrate. However, reversible aggregation with the pH was observed. Surprisingly, this control was not directly related to the surface charge like in water but to the solvent quality for the polyelectrolyte. This study is the first report on the use of the pH to tune the dispersion state of nanoparticles in an ionic liquid. It provides a better understanding of the mechanisms responsible for colloidal stability in ionic liquids.

Keywords

Colloidal stability, nanoparticles, maghemite, ionic liquid, ethylammonium nitrate, surface charge, acid-base titrations, small angle x-ray scattering, polyelectrolyte, poly(acrylic acid)

* Corresponding author :

address : Université Pierre et Marie Curie - Paris 6, UMR8234, case courrier 51, 4, place Jussieu, 75252 PARIS Cedex 05, France

Fax: 00 (33) 1 44 27 32 28

Tel: 00 (33) 1 44 27 36 76

E-mail: veronique.peyre@upmc.fr

Highlights for the article “Controlling nanoparticles dispersion in ionic liquids by tuning the pH”

- * Maghemite nanoparticles were dispersed in an ionic liquid, ethylammonium nitrate.
- * The stability is ensured by a coating of poly(acrylic acid) on the particles.
- * The influence of pH in the ionic liquid on colloidal stability is investigated.
- * The pH effect on stability is due to changes of the solvent quality for the polymer.
- * An unexpected stability domain is observed at very acidic pH.

ACCEPTED MANUSCRIPT

INTRODUCTION

Ionic liquids (IL) are promising solvents with unique properties. Indeed, they are exclusively composed of ions, which brings specific characteristics such as non-volatility, non-flammability and high electric and thermal conductivities. This provides a great potential for lots of new applications. For instance, IL can be used as electrolytes in batteries or solar cells [Yang, 2006]. Moreover, their unique and finely tunable solvation properties make them reaction media of uttermost interest, in particular for nanoparticles (NP) synthesis of varied sizes and shapes [Lee, 2010].

In this work, we focus on nanoparticles dispersions in IL. Dispersing nanoparticles in IL is indeed a developing field of interest that provides promising multifunctional materials, for example for catalysis or to form physical gels [Bideau, 2011].

The control and understanding of the stability of such dispersions remains a challenging task to achieve. Indeed, colloidal stability is possible only if the interparticle attractions (van der Waals interactions...) are counterbalanced by repulsive forces. Among the latter, the electrostatic stabilisation often occurring in polar molecular liquids is likely to differ in IL where the ionic nature of the solvent causes a screening of the classical long-range repulsive interparticle interactions. The DLVO model is thus not relevant here [Ueno, 2008a, Rodríguez-Arco, 2011]. Previous studies demonstrated the role of steric repulsions due to a polymer layer [Jain, 2011, Ueno, 2008a, Zhao, 2006] or to the solvent structuring around the NP [Ueno, 2008b, Néouze, 2010, Oliveira, 2009, Gao, 2015] on the stabilisation of NP dispersions in IL. Although the long-range electrostatic interactions are not present in IL, the surface charge and its counter-ions have been demonstrated to play an important role in the colloidal stability, probably through solvent layering at the NP surface [Mamusa, 2014a, b, Mamusa, 2015]. We intend here to complete the understanding of the colloidal stability in IL by studying a model system: functionalised maghemite NP in ethylammonium nitrate (EAN). We chose EAN because it has been deeply studied and characterised [Benlhima, 1989, Atkin, 2007, Hayes, 2010]. It is a hydrophilic protic IL in which a pH can be defined and acid-base reactions can occur and lead to charge modifications. Maghemite NP were chosen for the same reason. They have been studied in water [Lucas, 2007, Cousin, 2003] as well as in various solvents [Lefebure, 1998, Mériquet, 2003]. Moreover, using magnetic NP provides one more tool to adjust the interparticular interactions through the dipolar magnetic interaction (*via* the size or the chemical nature of the NP) [Cousin, 2003]. In addition, a remote actuation can be exerted with the application of an external magnetic field. The

individual extensive characterisations of both separated components provide a good basis for this study.

We studied the stabilisation and the state of dispersion of NP coated by a polyelectrolyte, poly(acrylic acid). In water, the colloidal stability obtained for such poly(acrylic acid) coated NP is due to electrostatic repulsive interactions when the polymer chains are deprotonated, at basic pH. At acidic pH, they are fully protonated and steric interactions are the only remaining repulsive interparticular interactions [Sehgal, 2005, Fresnais, 2013]. The switch from one interaction to the other can then be finely tuned with the pH. We aim at comparing the effect of these interactions in water and in EAN.

MATERIALS AND METHODS

Nanoparticles synthesis

Bare nanoparticles (BNP) of maghemite ($\gamma\text{-Fe}_2\text{O}_3$) were synthesised and obtained as an aqueous dispersion by coprecipitation following Massart's synthesis [Massart, 1981]. The BNP size polydispersity was then reduced by size sorting based on selective flocculation of the biggest BNP by increase of the ionic strength [Lefebure, 1998] to get two batches of approximately 6 nm diameter and 11 nm diameter BNP.

The size and polydispersity of each batch of BNP were routinely characterised by TEM. The analysis of the pictures lead to a log-normal size distribution of diameter 6.1 nm and a sigma value of 0.33 (*i.e.* an average surface of 145 nm² according to a first moment calculation on the distribution) for the smallest BNP (fig. 1) and a log-normal size distribution of diameter 11.4 nm and sigma value of 0.33 for the biggest BNP (see SI-1). The analysis of magnetisation measurements was coherent with these results (see SI-2 and SI-3). Since the results obtained afterwards for both batches of BNP do not differ significantly, we will focus on the smallest BNP in the following paragraphs. Small Angle X-ray Scattering results for the biggest BNP are reported in the supporting information only (SI-9 and SI-10).

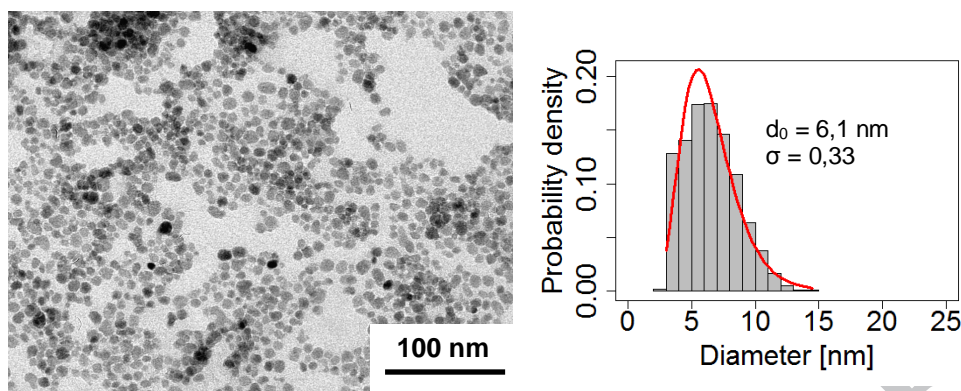


Figure 1: Left: TEM picture of the BNP; right: size distribution obtained by TEM pictures analysis (red line: log-normal distribution model, with $d_0 = 6.1 \text{ nm}$ and $\sigma = 0.33$)

The concentration of maghemite was measured using two techniques. The measurements of the iron content (after dissolution of the NP by concentrated HCl) were performed by flame atomic absorption spectroscopy (Aanalyst 100, Perkin-Elmer). The maghemite content was also obtained by UV-visible spectroscopy with the help of a master-curve (between 450 and 700 nm, see SI-4) for dispersions diluted in water (Avaspec 2048/Avalight DHC, Avantes). Both methods lead to coherent results.

Nanoparticles coating

Size sorted BNP were coated with a polyelectrolyte, polyacrylate, PAA^- (sodium salt, 2100 g mol^{-1} , Sigma-Aldrich, used as received). Functionalisations were performed by precipitation-redispersion in water following the procedure described in [Sehgal, 2005]. After redispersion and dialysis against distilled water, dispersions of PAA-coated NP (CNP) were obtained at $\text{pH} \approx 7-9$, with ammonium as counterions for the negatively charged acrylate groups. The dialysis step eliminates any residual free polymer chain in solution. The adsorption of PAA^- on BNP is irreversible [Sehgal, 2005], unlike the widely used citrate ligand which can be desorbed by dialysis of the free citrate ions. A repartition of two polymer chains and twenty-one titrable groups per square nanometre at the surface of the particles were measured on comparable NP in [Fresnais, 2013]. The effect of a longer PAA^- chain (8000 g mol^{-1}) was also studied. The results obtained for this longer chain are similar to those presented here. They are reported in the supporting information (SI-10 and SI-11).

In the following, we will refer to the polymer as PAA^- when it is mostly deprotonated, PAAH when it is mostly protonated and PAA when its protonation is not defined.

EAN synthesis and transfer of the particles

Ethylammonium nitrate was synthesised following the procedure described in [Evans, 1982 - Mamusa, 2014a]. Water content after analysis by Karl Fischer coulometric titrations is less than 0.3 wt. %. Aqueous solutions of CNP ($\Phi = 0.04$ to 0.15 vol. %) were then mixed with the same volume of dried EAN. Water was removed by freeze-drying in a dedicated apparatus (Christ Alpha 2-4 LD). The final content of water in the dispersions was estimated to be less than 2 wt. %. Due to the presence of particles, Karl Fischer titrations could not be used to determine the water content of the dispersions. It was observed that addition of basic water in any proportion to these dispersions in EAN had no effect on the colloidal stability, as checked by visual observation and dynamic light scattering. The water content is thus not a key parameter for colloidal stability of these systems.

pH measurements

pH measurements in EAN were carried out by potentiometric measurements between a dedicated glass electrode (Heito, high alkalinity) and a saturated calomel electrode connected to the solution by a salt bridge (agar-agar, KNO_3 , 2 mol L^{-1}) as in [Mamusa, 2014b]. Prior to any measurement, the response (electromotive force as a function of pH) of the electrode was determined according to three standards: a 0.10 mol L^{-1} solution of a strong base, tetramethylammonium hydroxide (TMAOH), in EAN, a 0.10 mol L^{-1} solution of a strong acid, benzenesulfonic acid (BSAc), in EAN and a 0.20 mol L^{-1} equimolar solution of benzoic acid and sodium benzoate ($\text{pK}_a = 5.4$) in EAN. The response of the electrode was linear with a slope equal to -56 ± 5 mV and was found to be constant during the whole titration. In what follows, strong acid and base (0.10 mol L^{-1} BSAc or TMAOH solutions) were used either to adjust the pH or for titrations. Please note that, in EAN, the auto-protolysis constant is equal to 10.0 ± 0.2 at 25°C [Benhlime, 1989 – Kanzaki, 2008]. Neutrality is then obtained at $\text{pH} = 5.0$.

Small angle X-ray scattering (SAXS)

Different dispersions were analysed by small angle X-ray scattering (SAXS) measurements on the SWING beamline of the SOLEIL Synchrotron (Saint Aubin, France). The measurements were performed at an energy of 7 KeV ($\lambda = 1.77$ Å), with a two dimensional CCD detector localised at a distance of 3.5 or 1 m from the sample in order to achieve a large q-range. Standard correction procedures were applied for sample volume, X-

ray beam transmission, empty cell signal subtraction and detector efficiency to obtain the scattered intensity in absolute scale (cm^{-1}). The software *Foxtrot*[®] was used to achieve such data reduction.

RESULTS

Transfer conditions on NP and PAA

The transfer of CNP from water to EAN was optimised regarding the pH values both in water and in EAN. Indeed, it was discovered that it is necessary to control precisely the pH of both solvents to get a stable dispersion of CNP in EAN after freeze-drying. For this study, obtaining a dark solution with no visible precipitate to the naked eye was used as a criterion of a stable dispersion, *i.e.* without aggregates larger than a few hundreds nanometres.

Optimised conditions consist in a neutral aqueous dispersion (pH = 6-8) and a very basic solution of EAN (pH = 9). CNP were transferred quantitatively and typical volume fractions of 0.1-0.2 vol. % were obtained. For more acidic or basic aqueous and/or EAN solutions, the dispersions obtained after freeze-drying ranged from flocculated to partially aggregated.

Bare nanoparticles could not be transferred quantitatively in EAN with this process. Only a very small amount (< 0.02 vol. %) of BNP get redispersed in EAN after freeze-drying, whatever the pH conditions.

In order to disperse free PAA⁻ chains in EAN in the same conditions as CNP, an aqueous solution of PAA⁻ was prepared and mixed with a basic solution of EAN (pH = 9). After freeze-drying, no precipitate could be observed.

Acid-base titrations

Titration of CNP dispersions ($\Phi = 0.13$ vol. %) were performed in water and in EAN. The objective is twofold: (i) explore the protonation behaviour of PAA⁻ in water and in EAN, free or grafted onto the NP, (ii) determine the PAA concentration after grafting.

Figure 2 presents pictures of the titrations of both kinds of dispersions at different pH. Starting from a basic dispersion in water or EAN (resp. *A1* and *B1*), acid solution is progressively added to the dispersions. It was chosen to wait for the stabilisation of the electromotive force (± 2 mV) (*i.e.* during a typical period of 1 to 5 minutes) between two additions in water, or for the stabilisation of the electromotive force (± 10 mV) (5 to 10 minutes) in EAN. In water, CNP aggregate progressively from about pH = 4 to pH = 3.5 (*A2-A3*) and the CNP remain then flocculated at lower pH (*A4*).

As for EAN solution, CNP display the same kind of behaviour at the beginning of the titration. They start to aggregate at approximately $\text{pH} = 7.2$ (*B2*) and the flocculation is complete at $\text{pH} = 6.7$ (*B3*) but, surprisingly, they redisperse at very low pH (*B4*). This redispersion indirectly shows that, as in water [Fresnais, 2013], the PAAH chains remain on the CNP, even when they are protonated. Indeed, as it was reported in the experimental part, uncoated NP do not form such dispersions and are flocculated at all pH in EAN.

It must be noticed that picture *B4* presented here shows a partial redispersion at $\text{pH} = 1.6$. However, a quicker acidification than the one performed during the titration would lead to a complete redispersion (see picture in supporting information, SI-5). Time plays an important role in this redispersion, as it can take several hours to occur in EAN when the pH has been slowly decreased. This redispersion at low pH never occurs in water.

In water and in EAN, starting from the flocculated domain, CNP redisperse when the pH is increased back to its initial basic value.

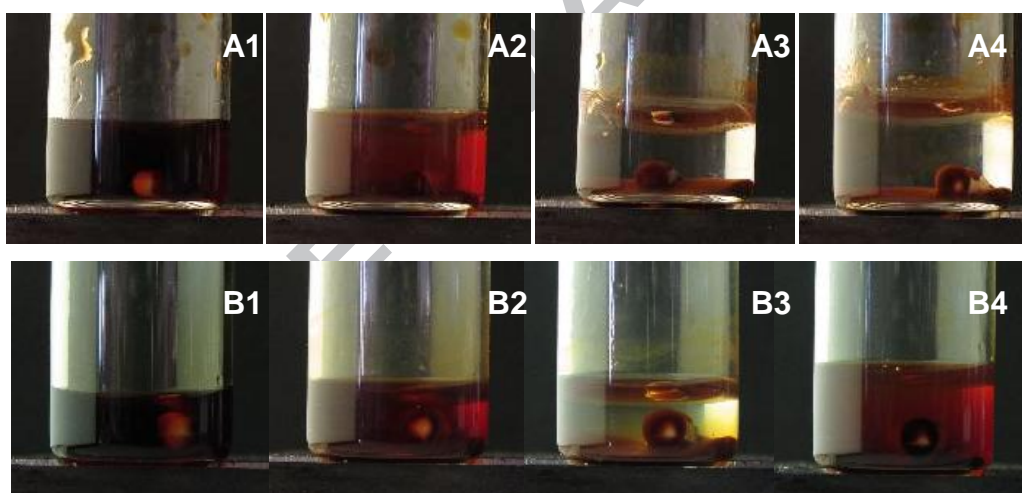


Figure 2: pictures of a sample put on a magnet while titrating. Above: CNP in water, $\text{pH} = 8.0 - 4.0 - 3.5 - 2.0$, beneath: CNP in EAN, $\text{pH} = 8.0 - 7.0 - 5.0 - 1.6$. The darker the dispersion, the more stable it is.

The curves displaying the pH versus the titration volume divided by the corresponding equivalent volume corresponding to figure 2 are plotted on figure 3. They are compared to the titration curves of PAA⁻ free chains in the same solvent (fig. 3, initial concentration of $2.4 \pm 0.2 \cdot 10^{-2} \text{ mol L}^{-1}$). In water, the curve obtained for free chains is similar to those reported in the literature [Laguecir, 2006]: it displays a nearly constant slope with a very smooth pH jump. This is characteristic of a polybase where the average pK_a depends on the protonation rate because of the intramolecular repulsions between adjacent carboxylate groups. During the

titration in water, no precipitate was observed in the free polymer solution. On the other hand, when grafted onto the NP, the titration curve of the polymer is more similar to that of weak monobases with a steeper pH jump at the equivalent volume. The environment of titrable acrylate groups is modified by the complexation of some of the monomers of the chains on the NP surface, thus modifying their apparent pKa.

Curves in EAN are not similar to those in water. Especially, free PAA⁻ chains in EAN display a different titration plot than expected for a polybase. Indeed, the steeper jump at the equivalent volume is more characteristic of a weak monobase titration. This is due to the screening of the intramolecular repulsion between carboxylates by the high ionic strength in the IL. In this case, the protonation of a carboxylate group becomes independent from the adjacent groups. While titrating, a flocculation of the polymer free chains in EAN can be seen between approximately pH = 6.5 and pH = 2 (see pictures in SI-6). The solution becomes clear again at pH < 2.

Given the unknown hydration rate of the polymer (estimated between 5 and 15 wt. %) and the uncertainty about the initial protonation rate, the exact initial concentration of protonable carboxylate groups is not precisely known *a priori*. The equivalent volume of the titrations, taken at the inflexion point on figure 3, leads to concentrations of $(2.9 \pm 0.2) 10^{-2} \text{ mol L}^{-1}$ for PAA⁻ free chains in EAN and $(1.8 \pm 0.2) 10^{-2} \text{ mol L}^{-1}$ in water. Since some base was added in EAN to dissolve the polyelectrolyte in the same conditions as the particles, this equivalent volume overestimates the concentration of protonable monomers. From the initial pH value, one can estimate the concentration of added base to be $4 \pm 2 10^{-3} \text{ mol L}^{-1}$, and thus the concentration of monomer is around $(2.5 \pm 0.4) 10^{-2} \text{ mol L}^{-1}$. These values are consistent with the added monomer concentration $((2.4 \pm 0.2) 10^{-2} \text{ mol L}^{-1})$ estimated from the manufacturer's information. As for the CNP dispersions, using the same argument, a protonable monomer concentration of $(1.5 \pm 0.7) 10^{-2} \text{ mol L}^{-1}$ is found for dispersions in EAN and $(2.0 \pm 0.2) 10^{-2} \text{ mol L}^{-1}$ in water. This approximately corresponds to 12 titrable monomers per square nanometre, which is in good agreement with previous results [Fresnais, 2013].

The half equivalence pH for free chains equals 5.8 ± 0.2 in water (in agreement with the value of 5.9 reported in literature [Laguecir, 2006] for similar polymers). This value is different from the pKa of an isolated monomer (e.g. pKa of ethanoic acid is 4.8 in water) because of the electrostatic interactions between the neighbouring groups in water [Overbeek, 1948]. The half equivalence pH for free chains in EAN is equal to 6.1 ± 0.4 in EAN. This value can be explained through the following reasoning. As we discussed in the previous paragraph, the titration of PAA⁻ in EAN is similar to a monobase titration. The half equivalence pH should then be equal to the pKa of the corresponding monomer in EAN,

which is 6.0 in EAN for ethanoic acid [Benlhima, 1989]. Indeed, a positive shift of the pKa is usually expected from water to EAN. This is due to the stronger acidity of nitric acid (HNO_3), *i.e.* the solvated proton in EAN, compared to hydronium (H_3O^+), the solvated proton in water [Kanzaki, 2008]. By way of comparison, we measured a pKa value of 5.8 ± 0.2 in EAN for acrylic acid (see SI-7) when 4.3 is reported in water.

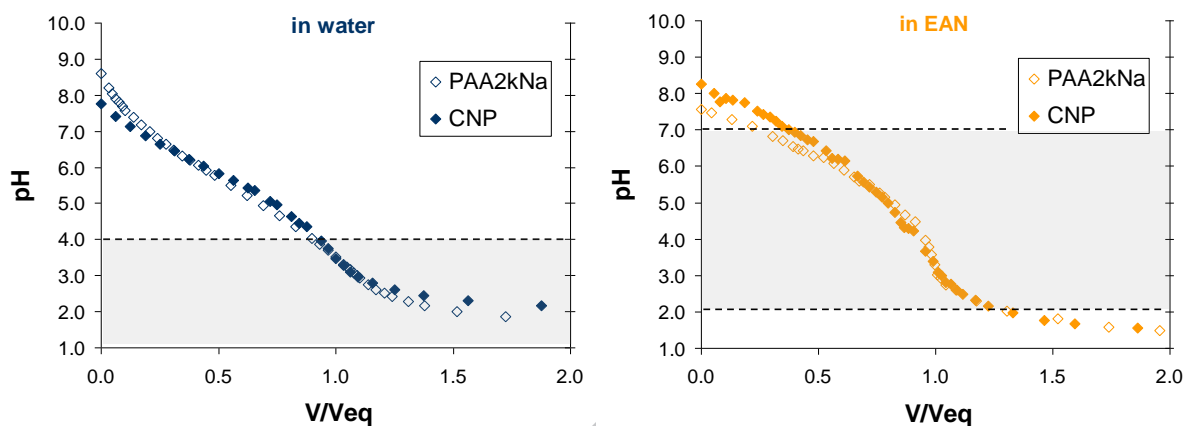


Figure 3: titration curves of PAA^- (hollow diamonds, monomers concentration: $2.4 \pm 0.2 \cdot 10^{-2} \text{ mol L}^{-1}$) and of CNP (filled diamonds, CNP volume fraction: $\Phi = 0.13 \text{ vol. } \%$); V/V_{eq} is the ratio of the volume of 0.10 mol L^{-1} BSAC solution added divided by the corresponding equivalent volume. The initial volume is $800 \mu\text{L}$ for each titration.

Left: aqueous solutions, right: EAN solutions, grey area: CNP flocculated domain.

SAXS

Some samples of CNP ($\Phi = 0.05$ to $0.1 \text{ vol. } \%$) along the titration curve in EAN and in water were analysed by SAXS. They were obtained by adding some BSAC solution to the basic dispersion except for the so-called “redispersed CNP” at basic pH. Indeed, this dispersion was achieved from a flocculated sample at an intermediate pH (pH = 3.9 in water, pH = 6.8 in EAN) to which a TMAOH solution was added. Their diffractograms are presented in figure 4 as the absolute intensity divided by the volume fraction versus the scattering vector, Q .

The dispersion of BNP ($\Phi = 0.1 \text{ vol. } \%$) in water at pH = 1.5 displays a diffractogram that can be fitted with a model of log-normal size distribution (diameter: 6.2 nm, sigma: 0.30, see SI-8) of spheres, $P(Q)$, which is coherent with the TEM data. It was used as a reference for the experimental form factor.

a) *Dispersions in water*

In water, diffractograms of CNP are similar from pH = 7.5 down to pH = 5.9 (not plotted on figure 4). They show a slight aggregation compared to BNP. The corresponding aggregation number can be calculated as the ratio of the extrapolated value of I/Φ for $Q = 0$ of the sample and of the BNP dispersion. A value of approximately 3 is obtained, which implies that these initial aggregates are relatively small. The further increase of the intensity at very low Q at lower pH is an indicator of bigger aggregates. According to the related diffractograms, increasing the pH of a flocculated dispersion leads to a redispersion of the aggregates. This redispersion is only partial since the initial dispersions at pH = 7.5 to 5.9 are not re-obtained, even if the pH is increased up to 10. The dispersion state obtained after the CNP redispersion is similar to the dispersion state at pH = 4.9.

b) *Dispersions in EAN*

In EAN, the initial dispersion at pH = 7.9 exhibits a stronger aggregation than in water at pH = 5.9 and higher, as indicated by the high I/Φ value extrapolated for $Q = 0$. The aggregation number can indeed be estimated at 8.

When large aggregates are formed, they can be broken up by two processes: by increasing or decreasing the pH. Both methods lead to similar dispersions, as confirmed by the superimposable diffractograms at pH = 1.3 and pH = 7.9. This is not the case in water, where only an increase of the pH could break up the aggregates.

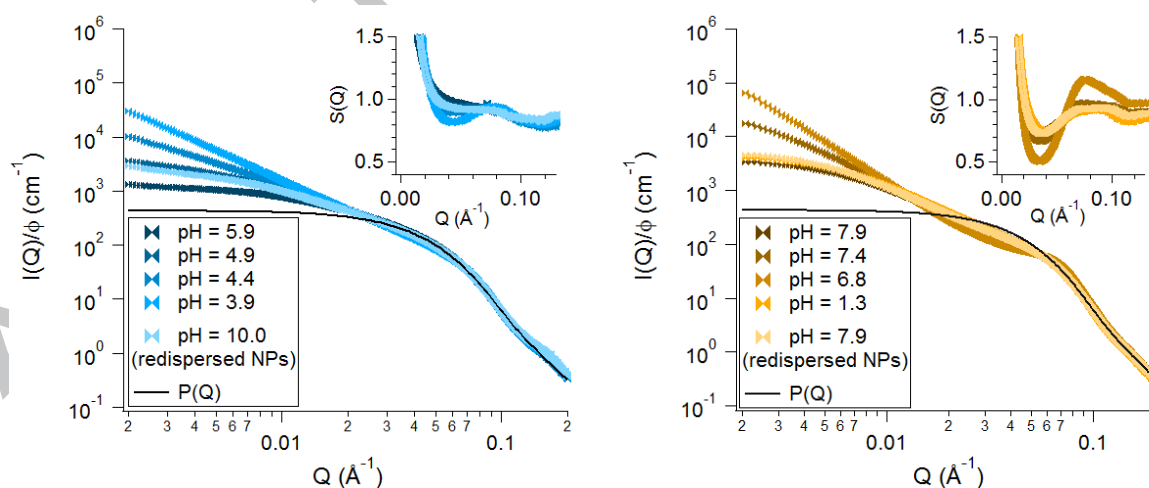


Figure 4: SAXS diffractograms of samples at different pH, normalised by the volume fraction of the different samples. Left: aqueous solutions, right: EAN solutions.

Insert: experimental structure factor obtained by dividing the normalised intensity by the experimental form factor (the BNP dispersion in water)

DISCUSSION

Colloidal stability and reversible aggregation: comparison water/EAN

These results show that the PAA coating is efficient to stabilise NP dispersions in EAN if the pH is carefully chosen and controlled. The dispersions are indeed stable over at least a year and the corresponding SAXS diffractograms do not evolve over this period (see SI-12). This observation demonstrates that this stability is not due to a kinetic slowing down resulting from the relatively high viscosity of EAN (“viscous stabilisation”) compared to water, but is indeed solvation stabilisation (Szilagyi, 2014).

In the following, we analyse and discuss the mechanisms responsible for the CNP colloidal stability in EAN.

a) Surface charge

In water, the colloidal stability and the tunable aggregation of the CNP with the pH can easily be explained by long-range electrostatic interactions. At high pH, the polymer layer at the CNP surface is charged and exerts a repulsive interaction on other CNP. When decreasing the pH, the carboxylate groups are neutralised by protonation. Thus, the repulsions between CNP weaken until the van der Waals and magnetic attractions between CNP prevail, which triggers the CNP aggregation. According to the titrations, it happens when most of the acid groups (approximately 90 %, by comparing with the equivalence) have been protonated and the surface charge is around 1.2 charge per square nanometre. This high level of charge neutralisation before flocculation can be understood using the concept of effective charge, Z_{eff} [Belloni, 1998, Oosawa, 1971, Manning, 1969], *ie* the apparent charge of the NP after electrostatic condensation of the counterions. Z_{eff} is more relevant to predict the interparticle repulsions whereas it is the structural charge, Z_{str} , that is modified by the titration. When Z_{str} is high (at the beginning of the titration), the ionic condensation is important (proportional to Z_{str}) and Z_{eff} is a constant (almost independent of Z_{str}). Colloidal stability is then obtained. Z_{eff} starts to decrease significantly only when Z_{str} is drastically reduced, leading to the NP aggregation at the same time.

In EAN, the titrations show that the flocculation of the CNP is triggered when less than 40 % have been neutralised (by comparing with the equivalence). The critical surface charge for the extensive aggregation of the CNP is then notably different (7.2 charges per square nanometre) from the one characterised in water, indicating that the stabilisation mechanism is completely different.

Moreover, in EAN, we demonstrated that, like in water, each monomer of PAA can be protonated only once. At very low pH, the surface of the CNP is then fully neutralised. The similarity of the diffractogram of the redispersed CNP at pH = 1.3 and at pH = 7.9 shows that the dispersions are similar for both conditions. It is thus an additional evidence that the surface charge is not the only parameter necessary to explain the colloidal stability in EAN.

b) Structure of the aggregates

Experimental structure factors of the dispersions in water and EAN were calculated (insert, figure 4), using the BNP dispersion in water ($\Phi = 0.1$ vol. %) as a reference for the form factor.

Regarding aqueous dispersions, the initial presence of small oligomers at basic pH could be due to a bridging of the particles by the same polymer chain or to the entanglement of polymer chains during the coating by precipitation. Upon a decrease of pH, aggregation can clearly be seen on these structure factors by the high $S(0)$ value. No sharp interaction peak emerges while aggregation occurs, which is likely to reveal very loose aggregates.

When the CNP are redispersed at basic pH after a flocculation at intermediate pH, the remaining oligomers could be due to a further irreversible entanglement of polymer chains that occurs during the precipitation at acidic pH.

In EAN, the formation of initial small oligomers could occur during the transfer process. Indeed, when EAN is added to the aqueous dispersion of CNP, the ionic strength is increased and the repulsive interactions between the carboxylate groups in water are screened, which enables the formation of aggregates. The diffractogram in EAN at pH = 7.9 looks rather similar to the one obtained in water at pH = 4.9. This suggests that the formations of small aggregates in water and in EAN are due to similar kinds of interactions between polymer chains in both solvents.

Besides, in EAN, the structure factor at pH = 6.8 displays an intense interaction peak around $Q^* = 0.075 \text{ \AA}^{-1}$, which is the reciprocal length of $d = 2\pi/Q^* = 8.4 \text{ nm}$. Given the SAXS particles size (6.2 nm), this contact distance can be modelled with a polymer layer thickness of 1.1 nm. It is coherent for a collapsed state of the polymer when an estimated polymer layer thickness of $(3 \pm 1 \text{ nm})$ in good solvent can be found in the literature (Fresnais, 2013).

These observations reveal two scales of aggregates. The smaller ones seem to be formed because of similar interactions and entanglements between the polymer chains in water and in EAN. On the contrary, the different structures of the big aggregates (loose in water, denser in EAN) demonstrate that they are formed through different mechanisms.

c) Solvent quality

In water, PAA chains are soluble at all pH. In EAN, we reported above the formation of a precipitate between pH = 6.5 and pH = 2. This shows that EAN is a poor solvent for PAA when the polymer chains are partially charged and a good solvent otherwise. Colloidal stability of the CNP follows the same trend. This correlation between the quality of the solvent for the coating polymer and the stability of the CNP dispersion was also discussed in another system [Ueno, 2008a, Ueno, 2014]. When EAN is a good solvent for the polymer, it creates a solvation sphere around the CNP. This sphere is certainly well structured and acts as a steric shell that prevents the CNP from aggregating. On the contrary, when EAN is a bad solvent for the coating polymer, the solvation of the CNP is less favourable than the interparticular aggregation, which leads to the CNP flocculation.

The evolution of the solvation quality of EAN for the PAA chains with the pH might be due to preferential hydrogen bonds between PAA chains or with the solvent depending on their protonation rate (figure 5). At basic pH, when the chains are fully deprotonated, the carboxylate groups can only form hydrogen bonds with the ethylammonium ions that are the only hydrogen donors in solution. When the chains are partially protonated, the interactions between carboxylic acid and carboxylate must be stronger than the possible interactions between these groups and the solvent ions. EAN becomes then a poor solvent for the polymer. At acidic pH, when all the groups of the polymer are protonated, the hydrogen bond between an hydrogen atom born by a carboxylic acid and a nitrate ion of the solvent is probably the most favourable bond. Indeed, nitrate ion is a better hydrogen acceptor than a carboxylic acid since it is charged. The transition from a regime where the bonds are established between the polymer chains (between pH = 6.5 and pH = 2) and a regime where they occur between a carboxylic group and ions from the solvent (pH < 2) probably takes time because of the slow ingress of the solvent ions in the collapsed polymer.

The slight difference of pH thresholds for CNP and free polymer chains flocculation can be attributed to a difference in the interactions between polymers if they are adsorbed at the NP surface or not.

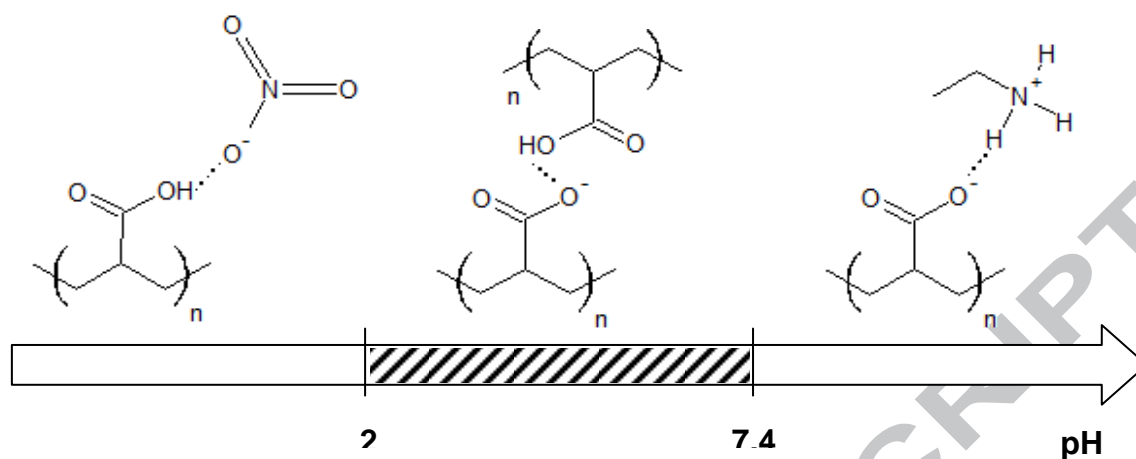


Figure 5: Most favourable hydrogen bonds as a function of the pH in EAN. The hatched zone indicates the flocculation domain.

CONCLUSION

In this work, we presented a comparison of the mechanisms responsible for the stability of PAA coated nanoparticles in water and in a protic ionic liquid, EAN. In water, the surface charge of the particles leads to repulsive interactions between them. The colloidal dispersion is then stable when the surfaces are sufficiently charged, which can be tuned by changing the pH.

In EAN, changing the pH still induces a modification of the polyelectrolyte charge through acid-base reactions, but the control of colloidal stability cannot be imputed to long-range electrostatic repulsion between charged objects. Indeed, the major influence of the charge modification appears to be the modification of the quality of the solvent for the nanoparticles coating. It could be related to the change of the nature and intensity of hydrogen bonding between the two protonation forms of acrylic acid and the two ions of the solvent. The solvation of the polymer is then different when the pH changes and this affects the colloidal stability of the nanoparticles. This leads to a surprising stability behaviour with three domains, a flocculation zone at intermediate pH and two stability domains at low and high pH.

This study provides new insights on the forces involved in colloidal stability of nanoparticles in an IL. Moreover, it highlights the very specific role of particles charge and solvation forces in EAN and the importance of mastering it through a careful pH control.

Aknowledgements

We acknowledge SOLEIL for provision of synchrotron radiation facilities and we would like to thank Dr. Javier Perez for assistance in using beamline SWING.

We would like also to thank Dr. Ryo Kanzaki and Dr. Fabrice Cousin for fruitful discussions.

References

- Atkin, R., Warr, G.G., 2007. Structure in Confined Room-Temperature Ionic Liquids. *J. Phys. Chem. C* 111, 5162–5168. doi:10.1021/jp067420g
- Belloni, L., 1998. Ionic condensation and charge renormalization in colloidal suspensions. *Colloids and Surfaces A: Physicochemical and Engineering Aspects* 140, 227–243. doi:10.1016/S0927-7757(97)00281-1
- Bideau, J.L., Viau, L., Vioux, A., 2011. Ionogels, ionic liquid based hybrid materials. *Chem. Soc. Rev.* 40, 907–925. doi:10.1039/C0CS00059K
- Cousin, F., Dubois, E., Cabuil, V., 2003. Tuning the interactions of a magnetic colloidal suspension. *Physical Review E* 68. doi:10.1103/PhysRevE.68.021405
- Evans, D.F., Yamauchi, A., Roman, R., Casassa, E.Z., 1982. Micelle formation in ethylammonium nitrate, a low-melting fused salt. *Journal of Colloid and Interface Science* 88, 89–96. doi:10.1016/0021-9797(82)90157-6
- Fresnais, J., Yan, M., Courtois, J., Bostelmann, T., Bée, A., Berret, J.-F., 2013. Poly(acrylic acid)-coated iron oxide nanoparticles: Quantitative evaluation of the coating properties and applications for the removal of a pollutant dye. *Journal of Colloid and Interface Science* 395, 24–30. doi:10.1016/j.jcis.2012.12.011
- Gao, J., Ndong, R.S., Shiflett, M.B., Wagner, N.J., 2015. Creating Nanoparticle Stability in Ionic Liquid [C4mim][BF4] by Inducing Solvation Layering. *ACS Nano* 9, 3243–3253. doi:10.1021/acsnano.5b00354
- Hayes, R., Warr, G.G., Atkin, R., 2010. At the interface: solvation and designing ionic liquids. *Phys. Chem. Chem. Phys.* 12, 1709–1723. doi:10.1039/B920393A
- Jain, N., Zhang, X., Hawke, B.S., Warr, G.G., 2011. Stable and Water-Tolerant Ionic Liquid Ferrofluids. *ACS Appl. Mater. Interfaces* 3, 662–667. doi:10.1021/am1012112
- Kanzaki, R., Uchida, K., Song, X., Umebayashi, Y., Ishiguro, S., 2008. Acidity and Basicity of Aqueous Mixtures of a Protic Ionic Liquid, Ethylammonium Nitrate. *Analytical Sciences* 24, 1347–1349. doi:10.2116/analsci.24.1347
- Laguecir, A., Ulrich, S., Labille, J., Fatin-Rouge, N., Stoll, S., Buffle, J., 2006. Size and pH effect on electrical and conformational behavior of poly(acrylic acid): Simulation and experiment. *European Polymer Journal* 42, 1135–1144. doi:10.1016/j.eurpolymj.2005.11.023

Lee, C.-M., Jeong, H.-J., Lim, S.T., Sohn, M.-H., Kim, D.W., 2010. Synthesis of Iron Oxide Nanoparticles with Control over Shape Using Imidazolium-Based Ionic Liquids. *ACS Appl. Mater. Interfaces* 2, 756–759. doi:10.1021/am900769x

Lefebure, S., Dubois, E., Cabuil, V., Neveu, S., Massart, R., 1998. Monodisperse magnetic nanoparticles: Preparation and dispersion in water and oils. *J. Mater. Res.* 13, 2975–2981.

Lucas, I.T., Durand-Vidal, S., Dubois, E., Chevalet, J., Turq, P., 2007. Surface charge density of maghemite nanoparticles: Role of electrostatics in the proton exchange. *The Journal of Physical Chemistry C* 111, 18568–18576.

Mamusa, M., Sirieix-Plénet, J., Cousin, F., Perzynski, R., Dubois, E., Peyre, V., 2014a. Microstructure of colloidal dispersions in the ionic liquid ethylammonium nitrate: influence of the nature of the nanoparticles' counterion. *J. Phys.: Condens. Matter* 26, 284113. doi:10.1088/0953-8984/26/28/284113

Mamusa, M., Sirieix-Plénet, J., Cousin, F., Dubois, E., Peyre, V., 2014b. Tuning the colloidal stability in ionic liquids by controlling the nanoparticles/liquid interface. *Soft Matter* 10, 1097–1101. doi:10.1039/C3SM52733F

Mamusa, M., Plénet, J.S., Perzynski, R., Cousin, F., Dubois, E., Peyre, V., 2015. Concentrated assemblies of magnetic nanoparticles in Ionic Liquids. *Faraday Discuss.* doi:10.1039/C5FD00019J

Manning, G.S., 1969. Limiting Laws and Counterion Condensation in Polyelectrolyte Solutions I. Colligative Properties. *The Journal of Chemical Physics* 51, 924–933. doi:10.1063/1.1672157

Massart, R., 1981. Preparation of aqueous magnetic liquids in alkaline and acidic media. *IEEE Transactions on Magnetics* 17, 1247–1248. doi:10.1109/TMAG.1981.1061188

Mériguet, G., Dubois, E., Perzynski, R., 2003. Liquid–liquid phase-transfer of magnetic nanoparticles in organic solvents. *Journal of Colloid and Interface Science* 267, 78–85. doi:10.1016/S0021-9797(03)00572-1

Neouze, M.-A., 2010. About the interactions between nanoparticles and imidazolium moieties: emergence of original hybrid materials. *J. Mater. Chem.* 20, 9593–9607. doi:10.1039/c0jm00616e

Oliveira, F.C.C., Rossi, L.M., Jardim, R.F., Rubim, J.C., 2009. Magnetic Fluids Based on γ - Fe_2O_3 and CoFe_2O_4 Nanoparticles Dispersed in Ionic Liquids. *J. Phys. Chem. C* 113, 8566–8572. doi:10.1021/jp810501m

Oosawa, F., *Polyelectrolytes*, Dekker, New York, 1971.

Overbeek, J.T.G., 1948. The Dissociation and Titration Constants of Polybasic Acids. *Bull. Soc. Chim. Belges* 57, 252–261. doi:10.1002/bscb.19480570416

Rodríguez-Arco, L., López-López, M.T., González-Caballero, F., Durán, J.D.G., 2011. Steric repulsion as a way to achieve the required stability for the preparation of ionic liquid-based

ferrofluids. *Journal of Colloid and Interface Science* 357, 252–254. doi:10.1016/j.jcis.2011.01.083

Sehgal, A., Lalatonne, Y., Berret, J.-F., Morvan, M., 2005. Precipitation–Redispersion of Cerium Oxide Nanoparticles with Poly(acrylic acid): Toward Stable Dispersions. *Langmuir* 21, 9359–9364. doi:10.1021/la0513757

Szilagyi, I., Szabo, T., Desert, A., Trefalt, G., Oncsik, T., Borkovec, M., 2014. Particle aggregation mechanisms in ionic liquids. *Phys. Chem. Chem. Phys.* 16, 9515–9524. doi:10.1039/C4CP00804A

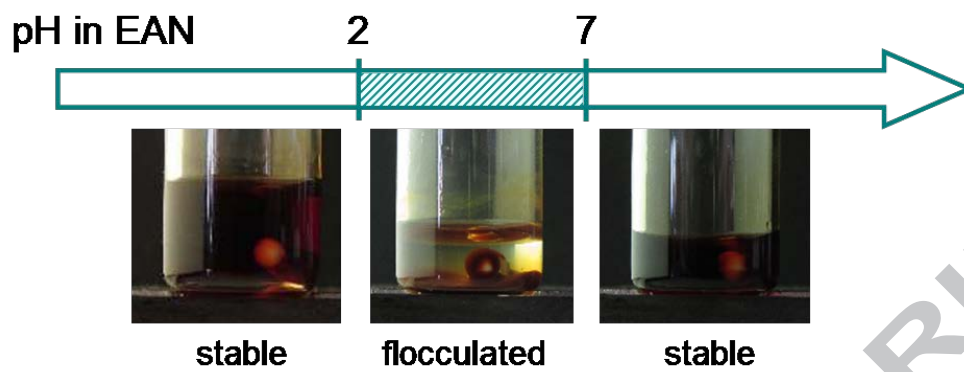
Ueno, K., Inaba, A., Kondoh, M., Watanabe, M., 2008a. Colloidal Stability of Bare and Polymer-Grafted Silica Nanoparticles in Ionic Liquids. *Langmuir* 24, 5253–5259. doi:10.1021/la704066v

Ueno, K., Hata, K., Katakabe, T., Kondoh, M., Watanabe, M., 2008b. Nanocomposite Ion Gels Based on Silica Nanoparticles and an Ionic Liquid: Ionic Transport, Viscoelastic Properties, and Microstructure. *J. Phys. Chem. B* 112, 9013–9019. doi:10.1021/jp8029117

Ueno, K., Fukai, T., Nagatsuka, T., Yasuda, T., Watanabe, M., 2014. Solubility of Poly(methyl methacrylate) in Ionic Liquids in Relation to Solvent Parameters. *Langmuir* 30, 3228–3235. doi:10.1021/la404797g

Yang, H., Yu, C., Song, Q., Xia, Y., Li, F., Chen, Z., Li, X., Yi, T., Huang, C., 2006. High-Temperature and Long-Term Stable Solid-State Electrolyte for Dye-Sensitized Solar Cells by Self-assembly. *Chem. Mater.* 18, 5173–5177. doi:10.1021/cm061112d

Zhao, D., Fei, Z., Ang, W.H., Dyson, P.J., 2006. A Strategy for the Synthesis of Transition-Metal Nanoparticles and their Transfer between Liquid Phases. *Small* 2, 879–883. doi:10.1002/smll.200500317



ACCEPTED MANUSCRIPT